Supporting Information:

Facet-Mediated Interaction between Humic Acid and TiO_2 Nanoparticle: Implications for Aggregation and Stability Kinetics in Aquatic Environment

Hui Zhang,[*,†] *Weimin Wang,*[†,‡] *Huanxin Zhao,*[‡] *Lixia Zhao,*[†] *Li-Yong Gan,*[§] *and Liang-Hong Guo*[†]

[†]State Key Laboratory of Environmental Chemistry and Eco-toxicology, Research Center for Eco-environmental Sciences, Chinese Academy of Sciences, 18 Shuangqing Road, Beijing 100085, China

[‡]Institute of Environmental and Safety Engineering, Shenyang University of Chemical Technology, Shenyang 110142, Liaoning, China

[§]School of Materials Science and Engineering, South China University of Technology, Guangzhou 510640, Guangdong, China

Aggregation Kinetics

The aggregation kinetics of nano-TiO_2 can be quantitatively described by the attachment efficiency α, which is defined as the ratio of the initial aggregation rate (k) at the given electrolyte concentrations to the aggregation rate constant under the diffusion-limited aggregation conditions (k_{fast}):[1]

$$\alpha = \frac{k}{k_{\text{fast}}} = \frac{\frac{1}{N_0}\left(\frac{\mathrm{d}R_h(t)}{\mathrm{d}t}\right)_{t\to 0}}{\frac{1}{N_{0,fast}}\left(\frac{\mathrm{d}R_h(t)}{\mathrm{d}t}\right)_{t\to 0,\text{fast}}} \qquad (1)$$

where N_0 is the initial TiO_2 concentration. $R_h(t)$ is the hydrodynamic radius at time t. The initial aggregation period is defined as the time period from the initial aggregation (t_0, R_{h0}) to the time $R_h \approx 1.4R_{h0}$. The critical coagulation concentration (CCC) was calculated at the intersection of the reaction-limited and diffusion-limited stability curves, which obtained by linear regression of α to electrolyte concentrations.

Determination of the percentage of the predominant facet

Based on the crystal model, the percentage of the exposed {101} facet and {001} facet in TiO_2 nanocrystals can be calculated by the geometrical parameters of the as-prepared crystals, which can be obtained from TEM images statistic.

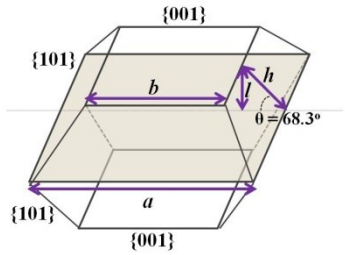

Figure S1. The geometrical models of anatase TiO_2 crystals.

The percentage of the {101} facet and {001} facet is calculated by the following equation:

$$S_{101} = \frac{a+b}{2} h = \frac{(a+b)l}{2\sin\theta}$$

$$S_{001} = b^2$$

$$P_{101}(\%) = \frac{8S_{101}}{8S_{101} + 2S_{001}} \times 100\%$$

$$P_{001}(\%) = \frac{2S_{001}}{8S_{101} + 2S_{001}} \times 100\%$$

The percentage of the predominant {101} facet and {001} facet in {101} TiO_2 and {101} TiO_2 nanocrystals were calculated to be 93.1% and 74.7%, respectively.

DLVO calculation for TiO_2 nanocrystals interactions.

The interaction energy between the faceted TiO_2 nanocrystals was calculated following the classic Derjaguin−Landau−Verwey−Overbeek (DLVO) theory, which is equal to the sum of the electrostatic double layer repulsion $\Phi_{EDL}(h)$ and the van der Waals attraction $\Phi_{VDW}(h)$. Since {101} TiO_2 and {101} TiO_2 are both exposed with plane facet, a plate-plate system model is adopted to calculate the interaction energy, which can be calculated using the following equations:[2,3]

$$\Phi_{EDL}(h) = \varepsilon_0 \varepsilon_w k\psi^2 [\frac{1}{\sinh(kh)} + 1 - \coth(kh)] \quad (1)$$

$$\Phi_{VDW}(h) = -\frac{A_{121}}{12\pi h^2} \quad (2)$$

$$\Phi_T = \Phi_{DLVO} = \Phi_{EDL}(h) + \Phi_{VDW}(h) \quad (3)$$

where ε_0 and ε_w are permittivity of vacuum (8.854×10^{-12} C V^{-1} m^{-1}) and relative

dielectric constant of water (78.5), respectively. ψ is the surface potential (V). h is the separation distance between the faceted TiO_2 nanocrystal (m). A_{121} is the Hamaker constant of anatase TiO_2 in water (3.5×10^{-21} J). k^{-1} is the Debye length (nm) and calculated by the following equation:

$$k^{-1} = \sqrt{\frac{\varepsilon_0 \varepsilon k_B T}{2 N_A e^2 I}} \quad (4)$$

where k_B is the Boltzmann's constant (1.38×10^{-23} J K^{-1}). T is the absolute temperature (K). N_A Avogadro's constant (6.02×10^{23} mol^{-1}). e is isolated unit electron charge (1.602×10^{-19} C). I is the ionic strength (mol L^{-1}).

References:

(1) Elimelech, M.; Gregory, J.; Jia, X.; Williams, R. A. Particle Deposition and Aggregation: Measurement, Modeling, and Simulation. Butterworth-Heinemann: Woburn, MA, **1995**.

(2) Brant, J. A.; Childress, A. E. Assessing Short-range Membrane−Colloid Interactions Using Surface Energetics. *J. Membr. Sci.* **2002**, *203* (1), 257−273.

(3) Tang, H.; Zhao, Y.; Yang, X. N.; Liu, D. M.; Shao, P. H.; Zhu, Z. G.; Shan, S. J.; Cui, F. Y.; Xing, B. S. New Insight into the Aggregation of Graphene Oxide Using Molecular Dynamics Simulations and Extended Derjaguin–Landau–Verwey–Overbeek Theory. *Environ. Sci. Technol.* **2017**, *51* (17), 9674−9682.

Table S1. Physicochemical properties of the natural waters used in the stability experiments.

Natural waters	Conductivity ($\mu s\ cm^{-1}$)	pH	TDS[a] ($mg\ L^{-1}$)	TOC[b] ($mg\ L^{-1}$)
Kunming Lake	245	8.28	138.0	4.56
A Lake located at Olympic forest park	678	8.41	370.5	7.85
Wenyu River	683	7.97	350.5	4.97
Qinghe wastewater treatment plants effluent	768	8.19	423.0	2.49

[a]TDS (total dissolved solids) was measured based on the weight of the residue after evaporating water at 103 ^{o}C in a drying oven. [b]TOC (total organic carbon) was analyzed on a O.I TOC Analyzer (College Station, TX, USA).

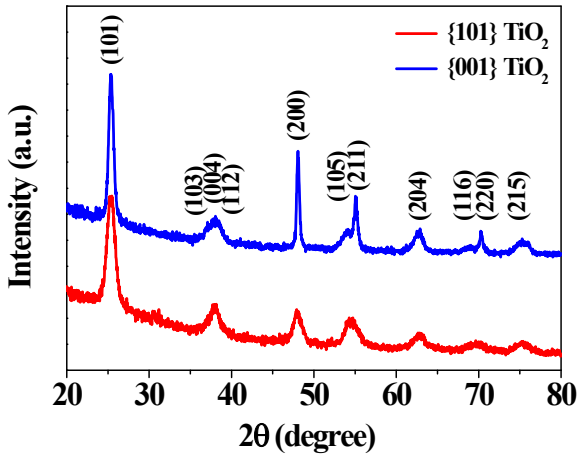

Figure S2. XRD patterns of the prepared {101} TiO_2 and {001} TiO_2 nanocrystals.

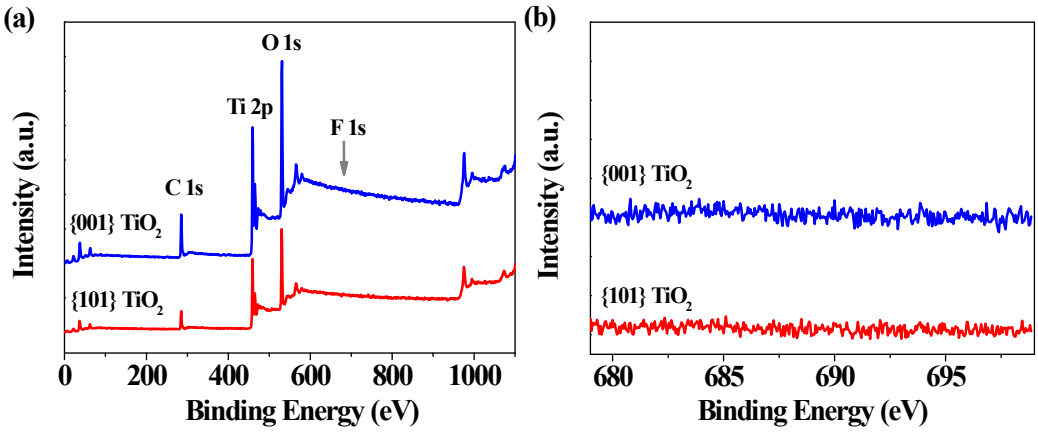

Figure S3. (a) XPS survey spectrum and (b) high-resolution F 1s XPS spectra of the prepared {101} TiO_2 and {001} TiO_2.

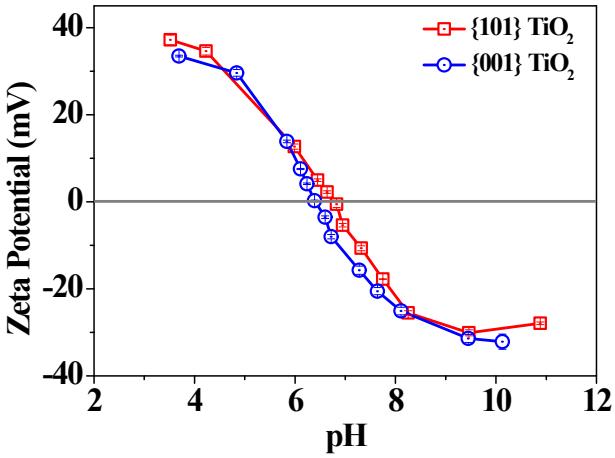

Figure S4. Variation of the Zeta potentials of {101} TiO_2 and {001} TiO_2 nanocrystal suspensions as a function of pH.

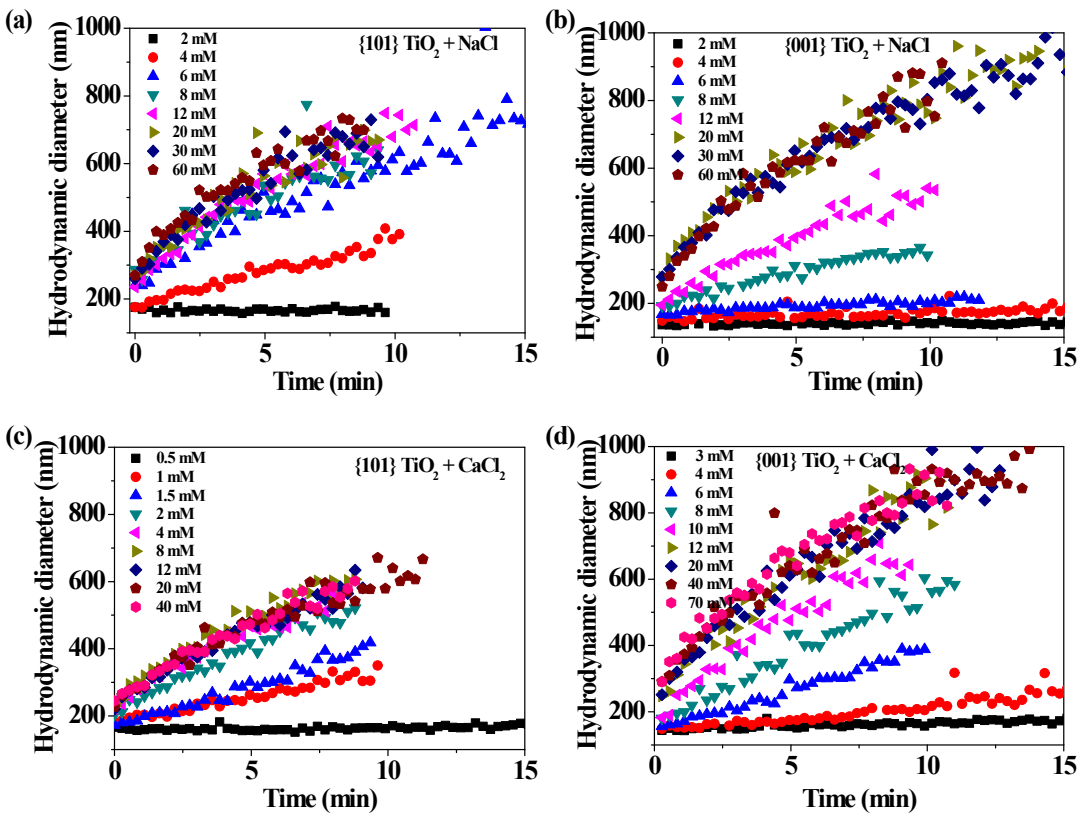

Figure S5. Representative aggregation profiles of (a,c) {101} TiO_2 and (b,d) {001} TiO_2 nanocrystals as a function of (a,b) NaCl and (c,d) $CaCl_2$ concentration. TiO_2 concentration was fixed at 20 mg L^{-1} and pH was maintained at 5.4 ± 0.1.

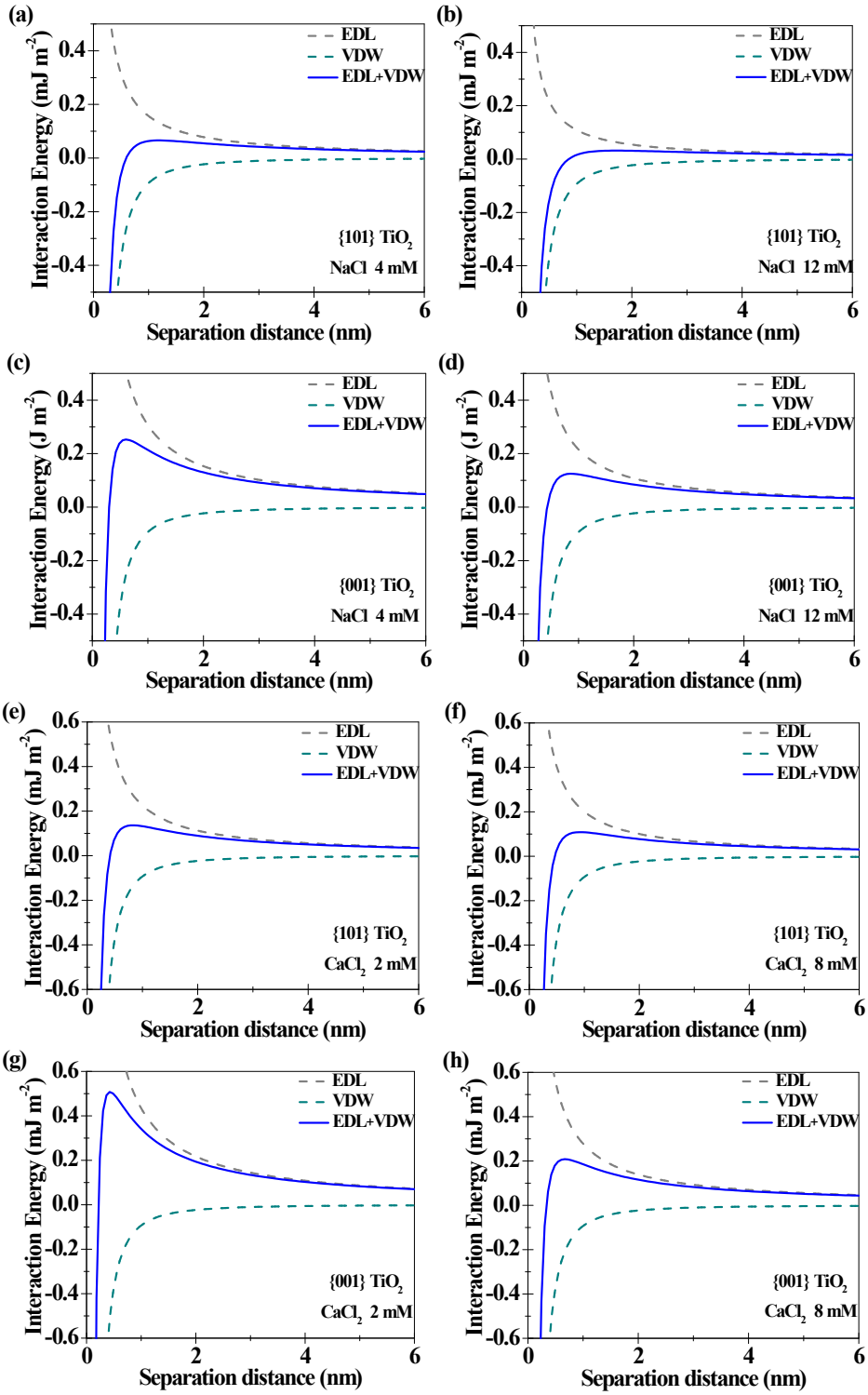

Figure S6. DLVO interaction profiles (including the electrostatic double layer repulsion (EDL), van der Waals attraction (VDW), and the net interaction energy) of {101} TiO_2 and {001} TiO_2 nanocrystals under different NaCl or $CaCl_2$ concentration.

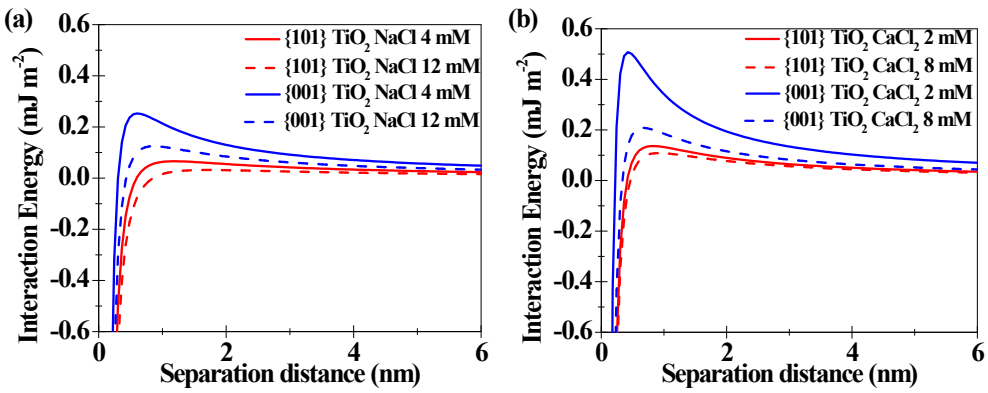

Figure S7. DLVO interaction energy profiles of the faceted TiO_2 nanocrystals in the presence of (a) NaCl and (b) $CaCl_2$ electrolyte.

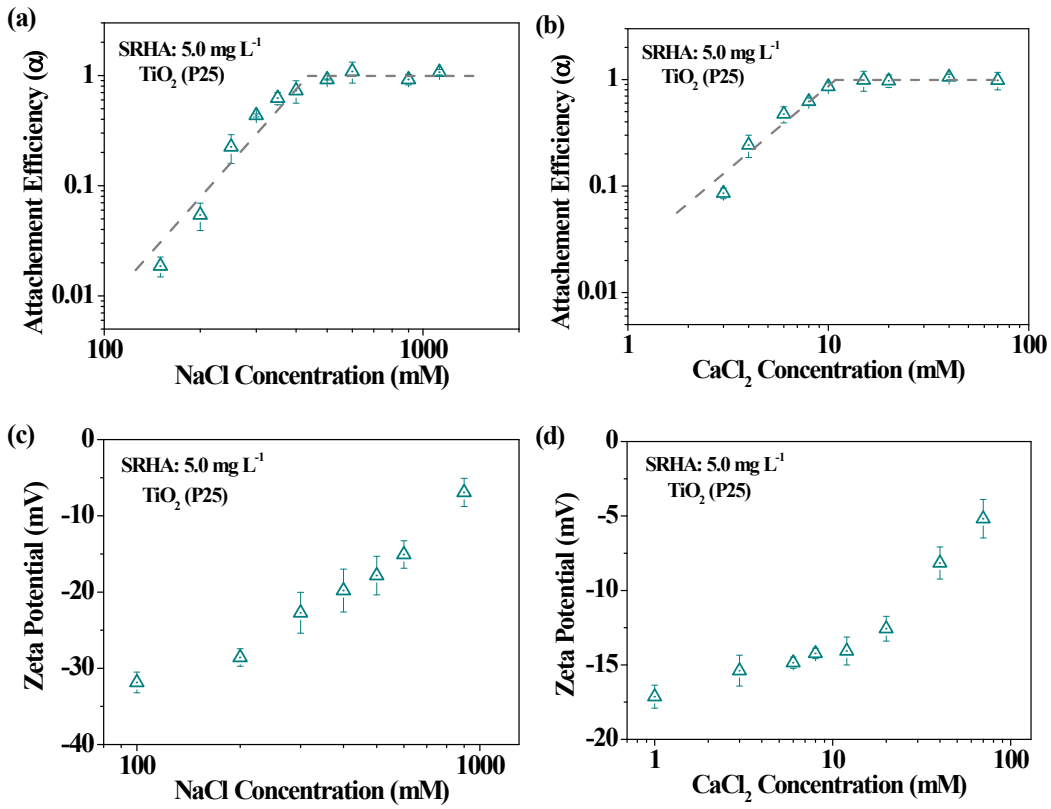

Figure S8. (a,b) Attachment efficiencies and (c,d) zeta potentials of TiO_2 (P25) as a function of (a,c) NaCl and (b,d) $CaCl_2$ concentration in the presence of 5.0 mg L^{-1} SRHA, respectively. Measurements were taken right after adding salt ions into the suspensions, and carried out at 25 ^{o}C, pH 5.4 ± 0.1.

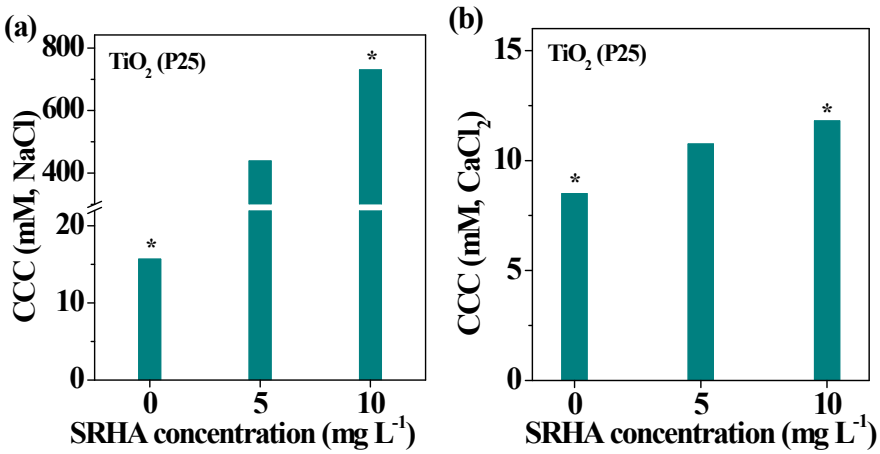

Figure S9. Effect of SRHA concentration (0 ~ 10.0 mg L^{-1}) on CCC of TiO_2 (P25) in (a) NaCl and (b) $CaCl_2$ electrolytes at pH 5.4 ± 0.1. *The data are adopted from our previous report: H. Zhang, J. Sun, L.-H. Guo. *NanoImpact,* 2016, *3-4*: 75-80.

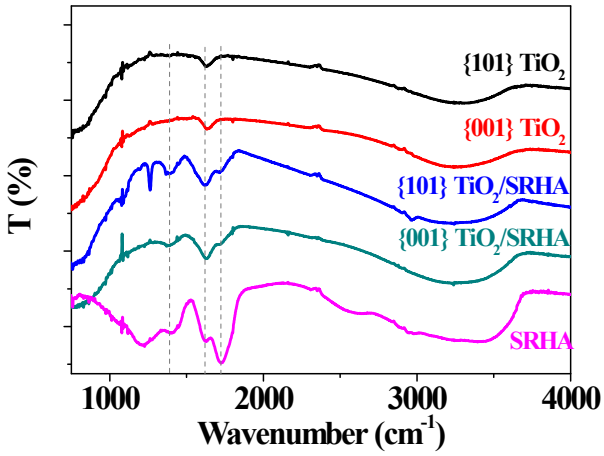

Figure S10. FTIR spectra of pristine {101} TiO_2 and {001} TiO_2 nanocrystals, pure SRHA, and the formed TiO_2-SRHA complex.